Nanoscale

Accepted Manuscript

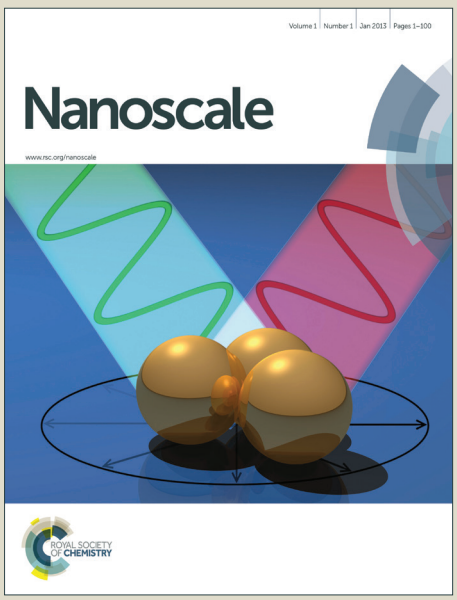

ROYAL SOCIETY OF CHEMISTRY

www.rsc.org/nanoscale

Search for Most Stable Structures of Silicon-Carbon Monolayer Compounds

Pengfei Li[1], Rulong Zhou[2]* and Xiao Cheng Zeng[1,3]*

[1] *Department of Chemical Physics, University of Science and Technology of China, Hefei, Anhui 230026, P. R. China*

[2]*School of Science and Engineering of Materials, Hefei University of Technology, Hefei, Anhui 230009, P. R. China*

[3]*Department of Chemistry and Nebraska Center for Materials and Nanoscience, University of Nebraska-Lincoln, Lincoln, Nebraska 68588*

*rlzhou@hfut.edu.cn; *xzeng1@unl.edu

Abstract

The most stable structures of two-dimensional (2D) silicon-carbon monolayer compounds with different stoichiometric compositions (i.e., Si:C ratio = 2:3, 1:3 and 1:4) are predicted for the first time based on the particle-swarm optimization (PSO) technique combined with density functional theory optimization. Although the 2D Si-C monolayer compounds considered here are rich in carbon, many low-energy metastable and lowest-energy silicon-carbon structures are not graphene (carbon monolayer) like. Phonon-spectrum calculations and *ab initio* molecular dynamics simulations are also performed to confirm dynamical stability of the predicted most stable 2D silicon-carbon structures as well their thermal stability at elevated temperature. Computed electronic band structures show that all three predicted silicon-carbon compounds are semiconductors with indirect bandgaps. Importantly, their bandgaps are predicted to be close to that of bulk silicon or bulk germanium. If confirmed in the laboratory, these 2D silicon-carbon compounds with different stoichiometric compositions may be exploited for future applications in nanoelectronic devices.

Introduction

Since the successful isolation of graphene sheets in 2004[1-5], this honeycomb structured 2D material has arose intensive research interests largely due to its remarkable electronic, mechanical, and optical properties, including unconventional quantum Hall effect, superior electronic conductivity, and high mechanical strength. The unique electronic properties of graphene in particular endow this 2D material as a potential candidate for applications in faster and smaller electronic devices. Like carbon, silicon is another group-IV element and also possesses a 2D allotrope with honeycomb structure, namely, the silicene. Unlike the graphene sheet which is flat, the silicene sheet exhibits a weakly-buckled local geometry[6-7]. Notwithstanding, the zero-bandgap characteristics of both graphene and silicene prevent direct use of both 2D sheets from undergoing controlled and reliable transistor operation, which hinder their wide applications in future optoelectronic devices. To date, much effort has been devoted to opening a bandgap (in 1.0 - 2.0 eV range) in either graphene or silicene sheets[8-12], although this is still a challenging task as it would require making some major changes in their intrinsic semi-metallic properties originated from the massless Dirac-fermion-like charge carriers.

The desire for continuous miniaturization of electronic devices calls for development of new and novel low-dimensional materials. Besides graphene and silicene, rich forms of 2D materials, particularly monolayer sheets with atomic thickness, have been reported in the literature. Coleman *et al.*[13] developed a liquid exfoliation technique that can efficiently produce monolayer 2D nanosheets from a variety of inorganic layered materials such as boron nitride (BN), molybdenum disulfide (MoS_2), tungsten disulfide (WS_2), molybdenum diselenide ($MoSe_2$) and molybdenum telluride ($MoTe_2$). Based on a modified liquid exfoliation technique, Xie *et al.* successfully fabricated monolayer vanadium disulfide (VS_2) and tin disulfide (SnS_2) in the laboratory[14-16]. On the theoretical side, increasing efforts have been undertaken in predicting structures and functional properties of novel 2D materials, for examples, monolayer boron sheets with low-buckled configurations[17,18],

monolayer boron-carbon (BC) compounds[19,20], boron-silicon (BSi) compounds[21], aluminum carbon (AlC) compounds[22], carbon nitride (CN)[23], germanene[24,25], tetragonal TiC[26], SnC[27] and other group III-VI compounds[27,28].

2D silicon-carbon (Si-C) monolayers can be viewed as composition-tunable materials between the pure 2D carbon monolayer – graphene and the pure 2D silicon monolayer – silicene. Efforts have been made on predicting most stable structures of the SiC sheet. Recently, Li *et al.* [29] and Zhou *et al.* [30] reported a metallic pt-SiC_2 2D sheet and semiconducting g-SiC_2 siligraphene, respectively, based on density functional theory (DFT) calculation. Their study indicates that electronic properties of 2D silicon-carbon compounds can be strongly dependent on the structure and stoichiometry. Moreover, few theoretical studies on 2D silicon-carbon compounds with different stoichiometry have been report in the literature. 2D silicon-carbon sheets with different stoichiometric compositions are expected to possess different electronic properties from SiC and SiC_2 sheets. Thus, it is timely to search for new 2D structures of silicon-carbon compounds with distinct stoichiometry and explore their structure-property relationship. In this study, we perform a comprehensive search for structures of 2D Si-C compounds with stoichiometric compositions (Si:C ratios) of 2:3, 1:3 and 1:4, using the particle-swarm optimization (PSO) techniques combined with density functional theory optimization. Our calculations suggest that the 2D Si-C compounds with richer carbon than silicon are energetically more favored. The predicted lowest-energy structures of Si_2C_3-I, SiC_3-I and SiC_4-I exhibit semiconducting characteristics. Phonon-spectrum calculations and *ab initio* MD simulations further confirm dynamical and thermal stability of these lowest-energy 2D structures. Finally, we show that the computed elastic constants of Si-C sheets are between those of graphene and silicene, suggesting that these newly predicted 2D Si-C compounds also possess good elastic properties.

Computational methods

The search for the most stable structure of 2D Si-C compounds is performed using the CALYPSO package[31] which has been previously used to predict the most stable as well as low-energy metastable 2D and 3D solid-state structures of various elements and compounds at different pressures[32-37]. Specifically, in the structure search, the population size of each generation is set to be 40, and the number of generations is fixed to be 30. A population of 2D Si-C structures in the first generation is generated randomly with the constraint of symmetry. In the ensuing generations, 60% of the population is generated from the best (lowest-energy) structures in the previous generation by using the particle-swarm optimization (PSO) scheme and the other 40% is generated randomly to ensure diversity of the population. Local optimization including the atomic positions and lateral lattice parameters is performed for each of the initial structures.

The structure relaxation and total-energy calculation are performed using the VASP package[38] within the generalized gradient approximation (GGA). An energy cutoff of 450 eV and an all-electron plane-wave basis set within the projector augmented wave (PAW) method are used. A dense k-point sampling with the grid spacing less than $2\pi \times 0.04$ Å^{-1} in the Brillouin zone is taken. To prevent the interaction between the adjacent solid sheets, a 20 Å vacuum spacing is set along the $\vec{z}$ direction. For geometric optimization, both lattice constants and atomic positions are relaxed until the forces on atoms are less than 0.01 eV/ Å and the total energy change is less than 1×10^{-5} eV. Phonon spectra of the low-energy crystalline structures are computed using the VASP package coupled with the PHONOPY program[39]. The phonon spectrum calculation is to assure that the obtained 2D sheets entail no negative phone modes.

Results and Discussion

A. Predicted lowest-energy structures of 2D Si-C compounds and their dynamic stability

2D Si-C compounds with three different Si-C stoichiometric compositions are considered, namely, Si_2C_3, SiC_3 and SiC_4. The predicted lowest-energy structure for each stoichiometry is shown in Figure 1. For comparison, the low-energy metastable structures for each Si:C ratio are also shown in Figure 1. Here, we use Roman numeral I, II and III to denote the energy ranking of the low-lying solid structures (for example, Si_2C_3-I and Si_2C_3-II denote the lowest-energy and the second lowest-energy structure, respectively).

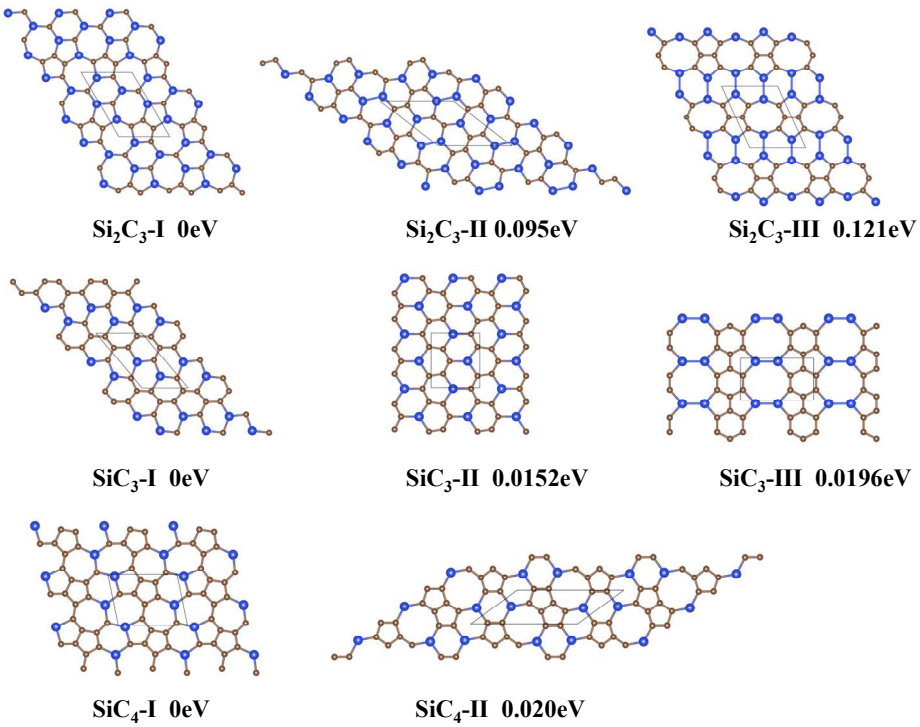

Figure 1 Predicted low-lying solid structures of 2D Si-C compounds based on the PSO simulations. C and Si atoms are represented by gray and blue spheres. Computed relative energy per atom with respect to the lowest-energy structure is given beneath each structure.

To evaluate relative stabilities among the predicted 2D C-Si compounds, we compute their cohesive energy. The formula of cohesive energy for the 2D systems is defined as follows:

$$E_{coh} = (xE_{Si} + yE_C - E_{Si_xC_y}) / (x + y)$$

where E_{coh} denotes the cohesive energy of 2D C-Si compounds, and E_{Si}, E_C and E_{SixCy}

are the total energy of a single Si atom, a single C atom, and the 2D Si_xC_y compound, respectively. Computed values of E_{coh} for all the predicted low-energy 2D Si_xC_y structure are listed in Table I. It can be seen that E_{coh} increases with increasing carbon composition. SiC_4 has the highest E_{coh} value, suggesting higher structural stability, compared to the other two C-Si sheets.

Table I. Computed cohesive energy of all the predicted low-energy C-Si sheets.

2D Structure	Cohesive Energy (eV/atom)
Si_2C_3-I	7.2660
Si_2C_3-II	7.1712
Si_2C_3-III	7.1446
SiC_3-I	7.8561
SiC_3-II	7.8409
SiC_3-III	7.8365
SiC_4-I	8.0631
SiC_4-II	8.0434

Next, to ensure that the predicted lowest-energy structure for each Si:C ratio is dynamically stable, phonon spectra of all three lowest-energy structures are computed using the supercell frozen phonon theory implemented in PHONOPY program. The computed phonon spectra of the lowest-energy structures of Si_2C_3, SiC_3 and SiC_4 (Si_2C_3-I, SiC_3-I and SiC_4-I) are plotted in Figure 2. Clearly, no negative phonon frequencies are present over the entire Brillouin zones for all three lowest-energy structures, indicating inherent dynamical stability of these 2D Si-C sheets.

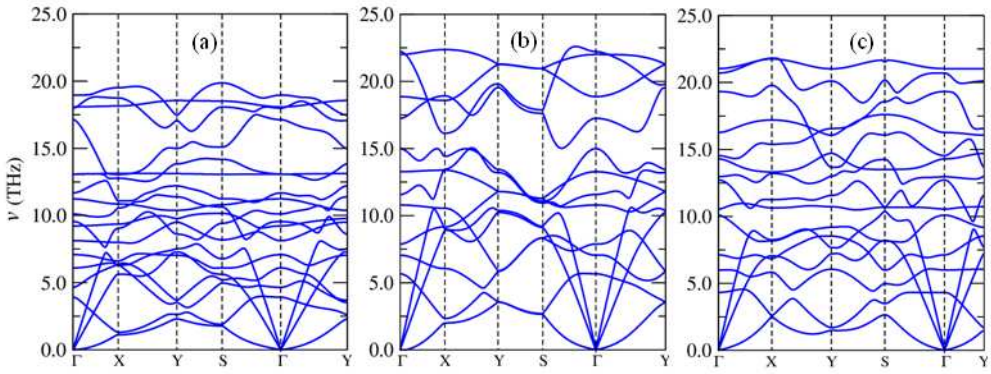

Figure 2 Computed phonon band structures of (a) Si_2C_3-I, (b) SiC_3-I and (c) SiC_4-I. Γ(0.0, 0.0, 0.0), X(0.5, 0.0, 0.0), Y(0.0, 0.5, 0.0) and S(0.5, 0.5, 0.0) refer to special points in the first Brillouin zone.

Moreover, thermal stability of Si_2C_3-I, SiC_3-I and SiC_4-I structures is examined using *ab initio* molecular dynamics (AIMD) simulations. In the AIMD simulation, the canonical ensemble (*NVT* ensemble) is adopted. The AIMD time step is 2 fs and the total simulation time is 15 ps for each given temperature. The structural features of each Si-C sheet prior to and after melting are shown in Figure 3. It can be seen that the equilibrium structures of Si_2C_3-I and SiC_3-I sheets at the end of 15 ps AIMD simulation show no sign of structural disruption at 3500 K, whereas both sheets exhibit disrupted structures at temperature 4000 K. Thus we can conclude that Si_2C_3-I and SiC_3-I structures can maintain their structure integrity and planar geometry below 3500 K. SiC_4-I sheet appears to have the highest thermal stability among the three structures as SiC_4-I can still keep its geometric structure over 15 ps AIMD simulation with temperature controlled at 4000 K.

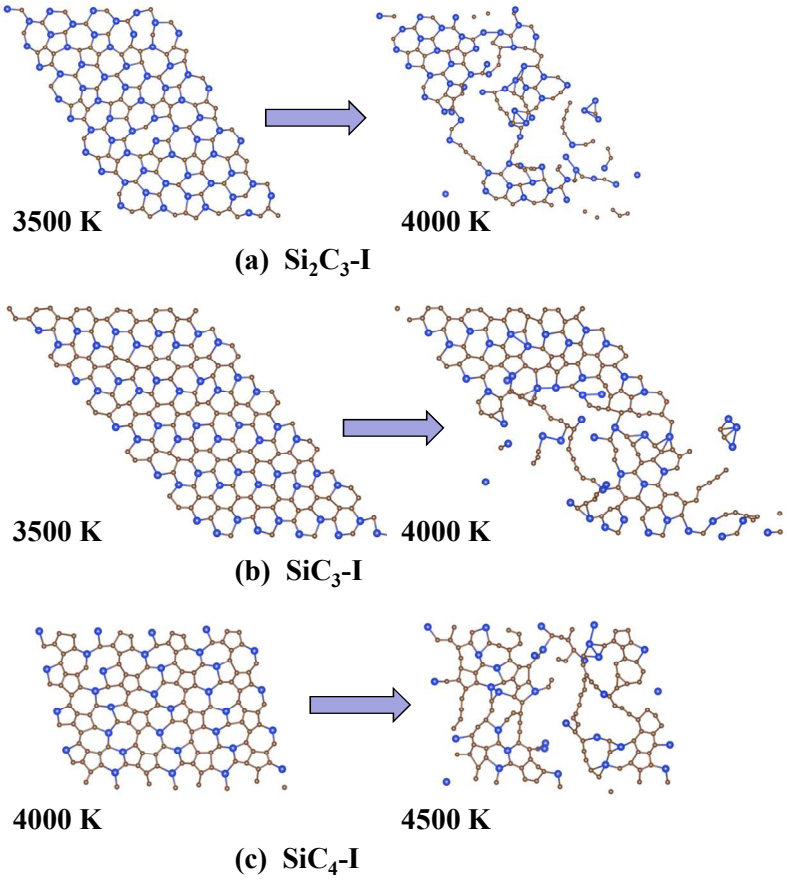

Figure 3 Snapshots of three lowest-energy 2D Si-C compounds at the end of two independent 15 ps AIMD simulations: (a) Si_2C_3-I, (b) SiC_3-I and (c) SiC_4-I sheets.

B. Detailed structures of three 2D Si-C compounds

a) Si_2C_3 sheets

Notice that all three Si-C 2D compounds with different stoichiometric composition are carbon-rich. As such, there are possibilities that their most stable structures may resemble the honeycomb structure of graphene. However, as shown in Figure 1, our global search suggests that many structures of these 2D Si-C compounds are quite different from that of the graphene. For Si_2C_3 sheet, the lowest-energy Si_2C_3-I exhibits a planar structure composed of pentagonal, hexagonal and heptagonal rings, where each hexagonal ring is surrounded by four heptagonal and two pentagonal rings (see Figure 1a). Each hexagonal ring is built upon three Si and three

C atoms, where Si and C atoms are located alternately on the vertices. There are two types of pentagonal rings: One is composed of three C and two Si atoms, while the other is composed of four C and one Si atoms. The heptagonal rings are all made of three Si and four C atoms. In all the polygonal rings, each Si atom is bonded with three C atoms within the same plane, representing a preference of the planar sp^2-bonding. No Si-Si bonds exist in the structure of Si_2C_3-I sheet.

The Si_2C_3-II sheet is 94.8meV/atom higher in energy than the Si_2C_3-I sheet, although all the polygonal rings in the Si_2C_3-II sheet are hexagonal. Notably, this Si_2C_3-II sheet can be viewed as silicon-doped graphene. Different from the Si_2C_3-I sheet where all the Si atoms are located separately (no Si-Si bonds in the sheet), there are both separately-distributed Si atoms and Si dimers in the Si_2C_3-II sheet. The percentage of Si atoms forming Si dimers is 50%. Since the sp^2-hybridization is not favored by silicon Si-Si bonds in a planar structure should be energetically unfavorable, which is possibly a main reason why Si_2C_3-II is less stable than Si_2C_3-I.

The third lowest-energy structure of Si_2C_3, namely the Si_2C_3-III sheet, is 121.4meV/atom higher in energy than the Si_2C_3-I sheet. Apparently, the Si_2C_3-III sheet is composed of pentagonal, hexagonal and octagonal rings, where each octagonal ring is surrounded by four pentagonal and four hexagonal rings. In this structure, all Si atoms form Si dimers so that its energy is much higher than that of Si_2C_3-I or Si_2C_3-II sheet.

b) SiC_3 sheets

For SiC_3, three 2D structures are found with close energies. The relative energies of SiC_3-II and SiC_3-III sheets are 15.2 and 19.6 meV/atom, respectively, with respect to the SiC_3-I sheet. Interestingly, the SiC_3-I sheet presents a graphene-like structure, which contains hexagonal rings only (see Figure 1d). Similar to the Si_2C_3-I sheet, each Si atom in the SiC_3-I sheet is bonded with three C atoms but not with Si atoms. The Si atoms along with the C atoms bonded with Si form armchair Si-C chains, while the other C atoms form armchair C chains. The Si-C chains and C chains connect with one another, forming the structure of the SiC_3-I sheet. The SiC_3-I sheet

can be viewed as a silicon-doped graphene. From the viewpoint of doping, it can be said that 50% A-site carbon atoms of graphene (in graphene, there are two inequivalent atomic sites, named as site A and site B) are substituted by silicon atoms. Note that our predicted SiC_3-I sheet is indeed the lowest-energy structure as recently predicted by Ding *et al*.[40]

The structure of SiC_3-II sheet is also graphene like[41]. Si atoms in the SiC_3-II sheet are also located separately as those in the SiC_3-I sheet (see Figure 1e). So, it is surprising that the SiC_3-II sheet is 15.2 meV/atom higher in energy than the SiC_3-I sheet. A closer examination of the structure indicates that the only difference between the structure of SiC_3-I and SiC_3-II sheets is the location of the two Si atoms in every hexagonal ring. In the SiC_3-I sheet, the two Si atoms are located at 1 and 3 sites of every hexagonal ring (we denote the six sites of any hexagonal ring as site 1 to site 6), while in the SiC_3-II sheet they are located at 1 and 4 sites. If from the viewpoint of doping, the SiC_3-II sheet can be viewed as that 25% A-site and 25% B-site carbon atoms of the graphene are substituted by Si atoms, respectively. The different location distribution of Si atoms leads to more C atoms connected with one another in the SiC_3-I sheet, compared to SiC_3-II, which should be the main reason why the SiC_3-I sheet has lower energy that the SiC_3-II sheet. Due to different Si distributions, the structure of SiC_3-II sheet cannot be decomposed into C chains and Si-C chains, while that of SiC_3-I sheet can.

The structure of SiC_3-III sheet is much different from those of the SiC_3-I and SiC_3-II sheets (see Figure 1f). The SiC_3-III sheet is composed of octagonal, hexagonal, and pentagonal rings, and it possesses a much higher symmetry compared to the SiC_3-I and SiC_3-II sheets. Si atoms in the SiC_3-III sheet form dimers while C atoms form complete hexagonal rings. It is known that Si dimers in a planar structure are energetically not favored whereas C hexagonal rings are favored inversely. So, even though Si-Si bonds exist, the total energy of the SiC_3-III sheet is merely a little higher than that of SiC_3-II sheet.

c) SiC_4 sheets

The lowest-energy structure of SiC_4, *i.e.* the SiC_4-I sheet, consists of pentagonal, hexagonal, and heptagonal rings, similar to the structure of the Si_2C_3-I sheet. Each hexagonal ring is surrounded by four heptagonal and two pentagonal rings. As shown in Figure 1g, the overall structure can be viewed as an alternate arrangement of two different chains: one is formed by heptagonal rings and another is formed by pentagonal and hexagonal rings. The SiC_4-II sheet has a similar structure as the Si_2C_3-III and SiC_3-III sheets, which contain pentagonal, hexagonal, and octagonal rings. However, unlike to the two structures, silicon dimers are not present in the SiC_4-II sheet. The cohesive energy of the SiC_4-II sheet is 19.7 meV/atom higher than that of the SiC_4-I sheet, due to the unfavorable octagonal rings in the 2D carbon systems.

Finally, we make a comparison of C-C/C-Si bond length in graphene/SiC and those SiC compounds. The bond length of C-C in Si_2C_3-I, SiC_3-I, and SiC_4-I is 1.438 Å, 1.455 Å, and 1.432 Å respectively, slightly longer than that in graphene (1.42 Å). For the C-Si bonds, they are slightly longer in Si_2C_3-I (1.792 Å) than those in SiC sheet (1.786 Å), but shorter than those in SiC_3-I (1.781 Å) and SiC_4-I (1.770 Å). We have also computed the Si-Si distance between two parallel stacked (in registry) Si_2C_3-I monolayers. As shown in Electronic Supplemental Information (ESI)[†] Figure S1, the minimum Si-Si distance is about 3.4 Å. Hence, new Si-Si bonds are not expected to form when two Si_2C_3-I monolayers are stacked on top of one another.

In summary, although the 2D Si-C compounds considered here are all C-rich, most of the lowest-energy structures and low-energy metastable structures are not akin to Si-doped graphene. Pentagonal and heptagonal rings occasionally are formed in the lowest-energy structures, and octagonal rings normally appear in the metastable structures. Si atoms tend to be located separated from one another, i.e. Si atoms prefer to be bonded with C atoms but not Si atoms, which is a main factor that influences relative stability of the 2D Si-C structures.

C. Electronic properties of 2D Si-C compounds

Computed electronic band structures of Si_2C_3-I, SiC_3-I and SiC_4-I sheets, based on GGA calculations, are plotted in Figure 4. It can be seen that all three lowest-energy structures are semiconducting, among which the Si_2C_3-I and SiC_3-I sheet possess a direct bandgap, while the SiC_4-I sheet exhibits an indirect bandgap. The computed bandgaps of Si_2C_3-I, SiC_3-I and SiC_4-I sheets (at GGA level) are 0.83 eV, 0.86 eV and 0.14 eV, respectively (see

Table **II**), all belonging to narrow-gap semiconductors. Note that GGA calculations tend to underestimate the bandgaps of semiconducting materials. To predict the bandgap of each Si-C compound more accurately, we also perform band-structure calculations using the HSE06 functional which has been proven to be more accurate for bandgap computation. The bandgaps of Si_2C_3-I, SiC_3-I and SiC_4-I sheets (based on HSE06 calculations) are 1.37 eV, 1.40 eV, and 0.51 eV, respectively. The bandgaps of Si_2C_3-I and SiC_3-I sheets are very close to that of bulk silicon, while the bandgap of SiC_4-I sheet is close to that of bulk germanium. Like bulk silicon and germanium, these 2D Si-C compounds may find applications in nanoelectronic devices.

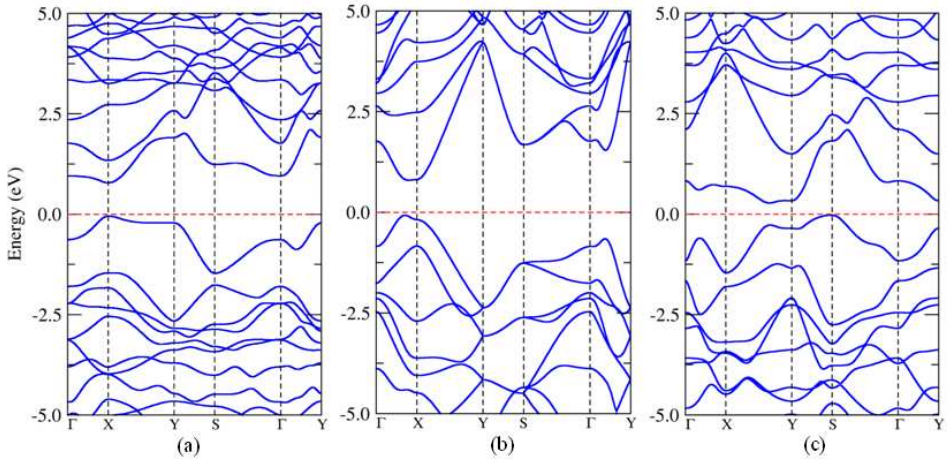

Figure 4 Computed electronic band structures of (a) Si_2C_3-I, (b) SiC_3-I and (c) SiC_4-I monolayer sheets. The Fermi level is set to 0 eV.

Table II Computed bandgaps of Si_2C_3-I, SiC_3-I and SiC_4-I monolayer sheets, based on

GGA and HSE06 calculations. Here, D and I denote direct and indirect bandgap, respectively.

2D Structure	Bandgap	
	GGA	HSE06
Si_2C_3-I	0.83 eV (D)	1.37 eV (D)
SiC_3-I	0.86 eV (D)	1.40 eV (D)
SiC_4-I	0.14 eV (I)	0.51 eV (I)

The computed partial density of states (PDOSs) of the predicted 2D Si-C compounds is also analyzed. The representative PDOS for Si_2C_3-I, SiC_3-I and SiC_4-I sheets is plotted in Figure 5. It is clear that in all three cases the higher valence bands and lower conduction bands (about -2.0 to 2.5 eV of the energy windows) are contributed by sp^2 orbitals of Si and C, while the p_z orbitals of Si and C only have contributions to the lower valence bands (below -2.0 eV) and higher conduction bands. So, the electronic properties of these sheets are only determined by the in-plane σ and σ^* bonds rather than π and π^* states, much different from graphene and graphite where the conjugate π states have major influence on the electronic properties such as excellent conductivity.

For the Si_2C_3-I sheet, it is clearly shown that the valence band maximum (VBM) is mainly contributed by the s, p_x and p_y orbitals of C atoms, where the contribution of Si is about a half of that of C. On the other hand, the conduction band minimum (CBM) is mainly contributed by Si atoms and the contribution of C atoms is also about a half of that of C. As for the SiC_3-I sheet, both the VBM and CBM are contributed mainly by the sp^2 hybridization states of C. And for the SiC_4-I sheet, it is obviously that the C and Si atoms contribute to the VBM and CBM nearly equally. It is worthy of noting that there is such a large difference in the contribution to the VBM and CBM states for different 2D Si-C compounds.

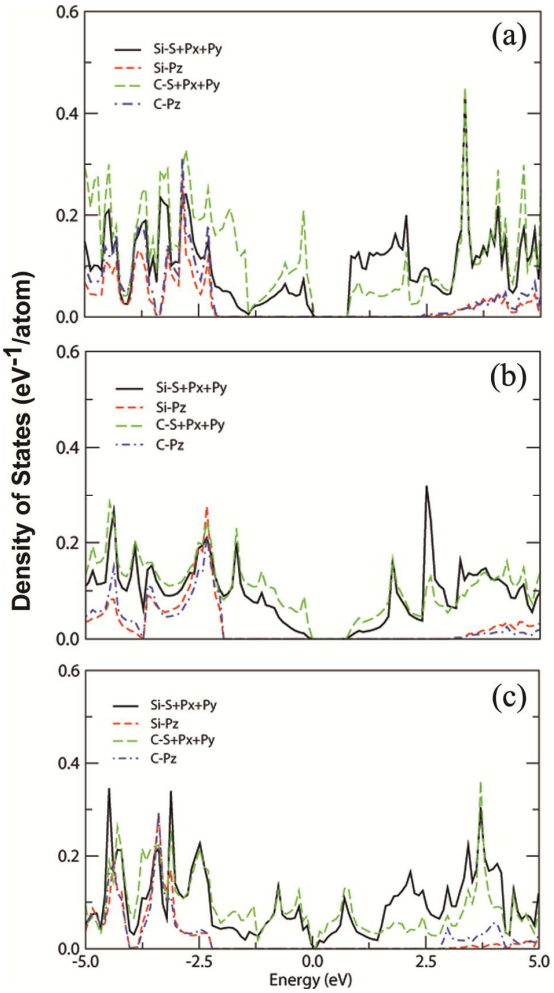

Figure 5 Computed PDOS for (a) Si_2C_3-I, (b) SiC_3-I and (c) SiC_4-I monolayer sheets. The Fermi level is set at 0 eV.

To gain deeper understanding of the bonding nature for the predicted 2D Si-C compounds, we take the electron localization function (ELF) analysis which can be used to classify chemical bonds rigorously. Due to the more localized characteristic of σ states than π states, the ELF distribution with a relatively large value (e.g., 0.725) for the Si-C compounds can mostly characterize the in-plane σ states. The plotted iso-surfaces of ELFs for the lowest-energy Si-C sheets are shown in Figure 6. It can be seen that in all the cases the ELFs of the C-C bonds are localized just at the center of the bonds and those of the Si-C bonds are localized closer to C atoms. This is due to the fact that the electronegativity of C atoms is stronger than that of Si atoms. For

the Si_2C_3-I sheet, apparently there are more Si-C bonds. The incline of ELFs to C atoms suggests that both VBM and CBM states are mainly originated from the in-plane sp^2 hybridization states of C and Si, respectively. For the other two cases, most C atoms connect with one another, forming C chains. The composition of Si-C bonds in SiC_3-I and SiC_4-I sheets are lower than that in the Si_2C_3-I sheet, hence the charge transferring from Si to C is weaker as reflected by the fact that the contribution of Si sp^2 states to the VBM is minor in both cases.

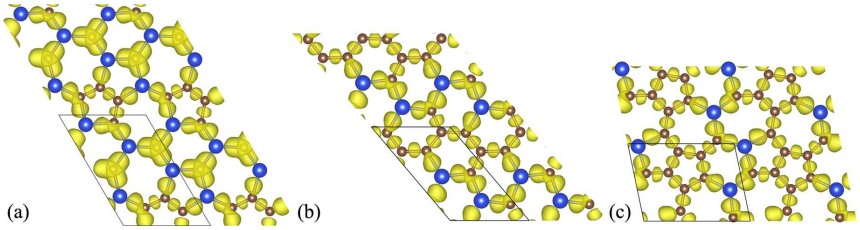

Figure 6 Iso-surface of ELF with the value of 0.725 for (a) Si_2C_3-I, (b) SiC_3-I and (c) SiC_4-I sheets.

D. Elastic properties of Si-C sheets

As mentioned above, the predicted lowest-energy structures of Si_2C_3, SiC_3 and SiC_4 sheets all possess excellent semiconducting properties that may be exploited for nanoelectronic applications. To this end, the mechanic strengths of the Si-C sheets are also important. It is well known that graphene possesses excellent elastic properties with large elastic constants: c_{11}=906.70 GPa and c_{12}=244.50 GPa. Previous studies have shown that silicene also has good elastic properties (c_{11}=287 GPa and c_{12}=127 GPa). We thus speculate that the predicted Si-C sheets may also own good elastic properties. Based on density functional theory calculation, elastic constants of these 2D Si-C compounds are computed (see Table III). To evaluate the specific value of elastic constants, we need to define interlayer spacing between two stacked Si_xC_y sheets. Here, we estimate it to be ~3.80 Å, which can be viewed as the thickness of a corresponding Si_xC_y bilayer. Since the interlayer interaction is van der Waals like, akin to that in graphite, this interlayer distance is just an estimated value due to the

limitation of DFT method in describing weak interaction. Four important elastic constants c_{11}, c_{12}, c_{22} and c_{66} of the three lowest-energy Si-C sheets are computed based on GGA. One can see that the computed c_{11} and c_{12} of the Si-C sheets are between those of graphene and silicene, and both tend to increase with the concentration of C atoms in the Si-C sheets. Hence, the SiC_4-I sheet possesses the largest value of c_{11} and c_{12} among the three Si-C sheets. However, the similar trend is not seen for c_{22} and c_{66}. The computed c_{22} and c_{66} of the SiC_3-I sheet are larger than those of Si_2C_3-I and SiC_4-I sheets. Overall, the predicted large elastic constants indicate that the 2D Si-C compounds possess reasonably good elastic properties.

Table III Computed elastic constants c_{11}, c_{12}, c_{22} and c_{66} for the predicted lowest-energy 2D Si-C compounds.

2D Structure	Elastic constants (GPa)			
	c_{11}	c_{12}	c_{22}	c_{66}
Si_2C_3-I	453.8	171.0	473.6	160.2
SiC_3-I	594.5	180.8	640.2	231.5
SiC_4-I	629.4	192.9	584.6	197.4

Conclusion

In conclusion, monolayer silicon-carbon (Si-C) materials can be viewed as composition-tunable materials between the pure 2D carbon monolayer – graphene and the pure 2D silicon monolayer – silicene. Based on the PSO algorithm combined with density functional theory optimization, we perform an extensive 2D-crystalline search of monolayer structures of silicon-carbon compounds. A number of low-energy structures are predicted for different stoichiometric compositions (i.e., Si_2C_3, SiC_3 and SiC_4). In the most stable structures, each Si atom is bonded with three C atoms, favoring the sp^2 hybridization. Dynamical and thermal stabilities of the predicted lowest-energy structures are examined through calculations of phonon dispersion and *ab initio* molecular dynamic simulations. These 2D Si-C compounds possess high

thermal stabilities such that the Si_2C_3-I and SiC_3-I sheets can retain their planar geometry below 3500 K while the SiC_4-I sheet can even maintain its planar structure up to 4000 K. Next, electronic and elastic properties of these three stable sheets are computed. Our calculations suggest that all the predicted lowest-energy Si-C sheets are semiconductors with a moderate bandgap ranging from 0.5 ~1.5 eV, comparable to that of bulk silicon or germanium. Lastly, we find these Si-C sheets possess reasonably large elastic constants whose values are typically between those of graphene and silicene. The composition dependent electronic and mechanical properties of 2D Si-C compounds may find applications in nanoelectronic devices.

Acknowledgements

RLZ thanks to the support of the National Natural Science Foundation of China (Grant No. 11104056), the Natural Science Foundation of Anhui Province (Grant No. 11040606Q33). XCZ is supported by ARL (Grant No. W911NF1020099), NSF (Grant No. DMR-0820521), and a grant from USTC for (1000 Talents Program) Qianren-B summer research.

References

[1] K. S. Novoselov, A. K. Geim, S. V. Morozov, D. Jiang, Y. Zhang, S. V. Dubonos, I. V. Grigorieva, A. A. Firsov, *Science* 2004, **306**, 666.

[2] K. S. Novoselov, A. K. Geim, S. V. Morozov, D. Jiang, M. I. Katsnelson, I. V. Grigorieva, S. V. Dubonos, A. A. Firsov, *Nature* 2005, **438**, 197.

[3] K. S. Novoselov, E. McCann, S. V. Morozov, V. I. Falko, M. I. Katsnelson, U. Zeitler, D. Jiang, F. Schedin, A. K. Geim, *Nat. Phys*. 2006, **2**, 177.

[4] Y. B. Zhang, Y. W. Tan, H. L. Stormer, P. Kim, *Nature* 2005, **438**, 201.

[5] Q. Tang, Z. Zhou, Z. Chen, *Nanoscale* 2013, **5**, 4541.

[6] A. Fleurence, R. Friedlein, T. Ozaki, H. Kawai, Y. Wang, Y. Yamada-Takamura, *Phys. Rev. Lett.* 2012, **108**, 245501.

[7] B. Feng, Z. Ding, S. Meng, Y. Yao, X. He, P. Cheng, L. Chen, K. Wu, *Nano Lett*. 2012, **12**, 3507.

[8] S. Y. Zhou, G. H. Gweon, A. V. Fedorov, P. N. First, W. A. de Heer, D. H. Lee, F. Guinea, A. H. Castro Neto, A. Lanzara, *Nat. Mater*. 2007, **6**, 770.

[9] L. Yang; C. H. Park, Y. W. Son, M. L. Cohen, S. G. Louie, *Phys. Rev. Lett.* 2007, **99**, 186801.

[10] H. J. Xiang, B. Huang, Z. Y. Li, S. H. Wei, J. L. Yang, X. G. Gong, *Phys. Rev. X* 2012, **2**, 011003.

[11] Z. Ni, Q. Liu, K. Tang, J, Zheng, J. Zhou, R. Qin, Z. Gao, D. Yu, J. Lu, *Nano Lett.* 2012, **12**, 113.

[12] S. Lebègue, M. Klintenberg, O. Eriksson, M. I. Katsnelson, *Phys. Rev. B* 2009, **79**, 245117.

[13] J. N. Coleman, M. Lotya, A. O. Neill, S. D. Bergin, P. J. King, U. Khan, K. Young, A. Gaucher, S. De, R. J. Smith, I. V. Shvets, S. K. Arora, G. Stanton, H.-Y. Kim, K. Lee, G. T. Kim, G. S. Duesberg, T. Hallam, J. J. Boland, J. J. Wang, J. F. Donegan, J. C. Grunlan, G. Moriarty, A. Shmeliov, R. J. Nicholls, J. M. Perkins, E. M. Grieveson, K. Theuwissen, D. W. McComb, P. D. Nellist, V. Nicolosi, *Science* 2011, **331**, 568.

[14] J. Feng, X. Sun, C. Wu, L. Peng, C. Lin, S. Hu, J. Yang, Y. Xie, *J. Am. Chem. Soc.* 2011, **133**, 17832.

[15] J. Feng, L. Peng, C. Wu, X. Sun, S. Hu, C. Lin, J. Dai, J. Yang, Y. Xie, *Adv. Mater.* 2012, **24**, 1969.

[16] Y. Sun, H. Cheng, S. Gao, Z. Sun, Q. Liu, F. Lei, T. Yao, J. He, S. Wei, et al. *Angew. Chem., Int. Ed.* 2012**, 51**, 8727.

[17] X. Yu, L. Li, X. W. Xu, C. C. Tang, *J. Phys. Chem. C* 2012, **116**, 20075.

[18] X. Wu, J. Dai, Y. Zhao, Z. Zhuo, J. Yang, X. C. Zeng, *ACS Nano* 2012, **6**, 7443

[19] X. J. Wu, Y. Pei, X. C. Zeng, *Nano Lett.* 2009, **9**, 1577.

[20] X. Luo, J. Yang, H. Liu, X. Wu, Y. Wang, Y. Ma, S. H. Wei, X. Gong, H. Xiang, *J. Am. Chem. Soc.* 2011, **133**, 16285.

[21] J. Dai, Y. Zhao, X.J. Wu, J.L. Yang, and X. C. Zeng, *J. Phys. Chem. Lett.* 2013, **4**,

561.

[22] J. Dai, X. J. Wu, J. L. Yang, and X. C. Zeng, *J. Phys. Chem. Lett.* 2014, **5**, 2058.

[23] H. J. Xiang, B. Huang, Z. Y. Li, S. H. Wei, J. L. Yang, X. G. Gong, *Phys. Rev. X* 2012, **2**, 011003.

[24] Z. Ni, Q. Liu, K. Tang, J. Zheng, J. Zhou, R. Qin, Z. Gao, D. Yu, J. Lu, *Nano Lett.* 2012, **12**, 113.

[25] A. O 'Hare, F. V. Kusmartsev, K. I. Kugel, *Nano Lett.* 2012, **12**, 1045.

[26] Z. Zhang, X. Liu, B. I. Yakobson, W. Guo, *J. Am. Chem. Soc*. 2012, **134**, 19326.

[27] H. Sahin, S. Cahangirov, M. Topsakal, E. Bekaroglu, E. Akturk, R. Senger, S. Ciraci, *Phys. Rev. B* 2009, **80**, 155453.

[28] C. Freeman, F. Claeyssens, N. Allan, J. Harding, *Phys. Rev. Lett.* 2006, **96**, 066102.

[29] Y. Li, F. Li, Z. Zhou, Z. Chen, *J. Am. Chem. Soc.* 2011, **133**, 900.

[30] L. Zhou, Y. Zhang, L. Wu, *Nano Lett.* 2013, **13**, 5431.

[31] Y. C. Wang, J. Lv, L. Zhu, Y. M. Ma, *Phys. Rev. B* 2010, **82**, 094116.

[32] Y. Ma, M. I. Eremets, A. R. Oganov, Y. Xie, I. Trojan, S. Medvedev, A. O. Lyakhov, M. Valle, V. Prakapenka, *Nature*, 2009, **458**, 182.

[33] A. R. Oganov, Y. M. Ma, Y. Xu, I. Errea, A. Bergara, A. O. Lyakhov, *Proc. Natl. Acad. Sci. USA*, 2010, **107**, 7646.

[34] Y. Xie, A. R. Oganov, Y. Ma, *Phys. Rev. Lett.* 2010, **104**, 177005.

[35] R.L. Zhou and X.C. Zeng, *J. Am. Chem. Soc.* 2012**, 134** , 7530.

[36] R. Zhou, B. Qu, J. Dai, and X. C. Zeng, *Phys. Rev. X* 2014**, 4**, 011030.

[37] J. Dai, X. J. Wu, J. L. Yang, and X. C. Zeng, *J. Phys. Chem. Lett.* 2013, **4**, 3484.

[38] G. Kresse, J. Furthmüller, *Phys. Rev. B*, 1996, **54**, 11169.

[39] A. Togo, F. Oba, I. Tanaka, *Phys. Rev. B*, 2008, **78**, 134106.

[40] Y. Ding, Y. Wang, *J. Phys. Chem. C*, 2014, **118**, 4509.

[41] Q. Tang, Z. Zhou, *Prog. Mater. Sci.*, 2013, **58**, 1244.